Electromagnetic Response Prediction of Reflectarray Antenna Elements Based on Support Vector Regression

Liping Shi, Qinghe Zhang, Shihui Zhang, Chao Yi, and Guangxu Liu

College of Computer and Information
China Three Gorges University, Yichang, 443002, China
1593735417@qq.com, zqh@ctgu.edu.cn

Abstract ─ In this letter, support vector regression (SVR) is used to predict the electromagnetic (EM) response of a complex shaped reflectarray (RA) unit cell. The calculation of the scattering coefficients of passive RA elements with periodic intervals is firstly transformed into a regression estimation problem, and then an analysis model is established by SVR to quickly predict the EM response of the unit cells. To this end, the full-wave (FW) simulation software is used to obtain a set of random samples of the scattering coefficient matrix of the RA antenna unit cell, which is used for SVR training. Under the same conditions, the radial basis function network (RBFN) is also used to predict the EM response of the elements, and the comparison results show the effectiveness and accuracy of the proposed method.

Index Terms ─ Electromagnetic response, reflectarray antenna elements, scattering matrix, support vector regression.

I. INTRODUCTION

Microstrip reflectarray (RA) antennas have replaced traditional parabolic reflectors and array antennas with advantages such as simple structure, easy manufacturing and transportation, and low manufacturing cost [1,2].

An important step in synthesizing such a high-performance RA antenna is to analyze its electromagnetic (EM) response. There are many different methods for the analysis of RA antennas. Considering the periodic characteristics of such antennas, the most commonly used method is the full-wave (FW) simulation which assumes the local periodicity [3,4]. Traditionally, a wide range of EM simulation software, such as High Frequency Structure Simulator (HFSS) and CST Microwave Studio [5], which used to calculate the RA unit cells' scattering matrix and establish *scattering matrix-versus-descriptors* lookup tables (LUTs) [6,7]. As we all know, the main disadvantage of establishing a database is that it requires a large number of samples and uses interpolation techniques [8], and the standard interpolation method cannot be used for EM prediction because of the high nonlinearity between the descriptor (frequency, angle of incidence, geometry, etc.) of the unit cell and the corresponding EM response [1,7,9]. Since the number of LUTs items increase exponentially with the degrees of freedom (DoFs) of the unit cells [6], involving a large amount of memory and computation time. In addition, parametric scanning is usually required to analyze the design of each possible cell, which is also very time-consuming [9]. Therefore, the FW method is rarely used in actual antenna synthesis [6].

The rapid development of machine learning methods has made it widely used in the field of antennas and electromagnetics. At present, there have been many successful applications including antenna diagnosis [10], modeling [11] and parameter reconstruction [12]. Several papers have used machine learning methods to design and analyze antennas. In [5,13], ANNs were used to design and analyze RA antenna and to predict magnitude, but the results were limited and overfitting problems may be encountered. In [7], Salucci, *et al* used the ordinary kriging (OK) based on statistical learning method to quickly predict the EM response of RA antenna. Inspired by this, support vector regression (SVR) has a large number of kernel functions that can be used compared to other regression methods, has a more solid mathematical theoretical foundation, and has the advantages of strong generalization ability and good robustness. Therefore, this paper intends to use SVR algorithm to predict the magnitude and phase response of RA antenna unit cells with complex shapes under different polarization states (i.e., co-polarization and cross-polarization), so as to overcome the problems of calculation time and memory of traditional FW simulation and the accuracy of ANNs.

The evaluation of the scattering coefficient of a typical RA antenna element characterized by arbitrary DoFs is first recast as a vectorial regression problem. Then, CST is used to simulate different RA antennas to obtain a set of data for SVR training and establish a substitute model. Finally, the results of SVR training are compared with the FW simulation results and the radial basis function network (RBFN), to prove the superiority

Submitted On: December 5, 2019
Accepted On: August 9, 2020
https://doi.org/10.47037/2020.ACES.J.351210

of the proposed method.

II. OVERVIEW OF RA ANALYSIS

Microstrip RA antenna comprises a planar reflective surface and a feeder that illuminates a passive array of microstrip patches and produces an induced current, which in turn properly focuses the reflected beam by controlling the scattering properties of the RA surface [2].

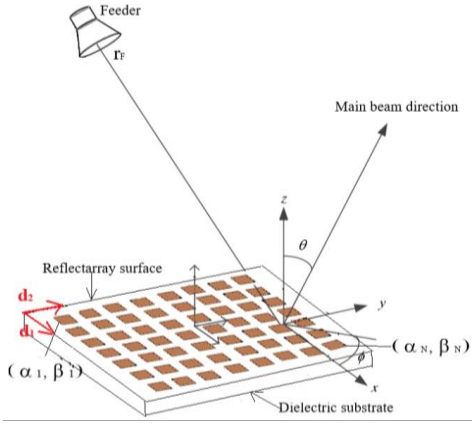

Fig. 1. Sketch of the RA antenna.

A microstrip RA consists of a planar array of $N\times N$ patches that are periodically arranged on a grounded single-layer dielectric substrate (Fig. 1). Each nth $(n=1,...,N^2)$ array element is described by I DoFs $\mathbf{L}(n)\triangleq\{L^{(i)}(n); i=1,...,I\}$. The field radiated by the RA, $\mathbf{E}(\theta,\varphi;\ f)$, is given by [7,14,15]:

$$\mathbf{E}(\theta,\varphi;\ f)=\sum_{n=1}^{N^2}\{[\mathcal{R}(\theta_n,\varphi_n;\ f)+\mathcal{S}(\theta_n,\varphi_n;\ f,\mathbf{L}(n))]\cdot\mathbf{E}_F(\theta_n,\varphi_n;\ f)\exp(jk_0\mathbf{r}_n\cdot\hat{\mathbf{r}})\},\quad(1)$$

where f is the working frequency, $\hat{\mathbf{r}}\triangleq(\sin\theta\cos\varphi,\ \sin\theta\sin\varphi,\cos\theta)$, $\mathbf{r}_n=(\alpha_n,\beta_n,0)$ is the location of the nth patch element, $k_0=(2\pi c_0)/f$ is the free-space wavenumber (c_0 being the speed of light), and (θ_n,φ_n) are the elevation angle and the azimuth one of the direction of incidence from the feed to the nth element, $\mathcal{R}(\theta_n,\varphi_n;\ f)=\{R_{xy}(\theta_n,\varphi_n;\ f);\ x,y=\{\theta,\varphi\}\}$ is the plane wave reflection matrix, $\mathcal{S}(\theta_n,\varphi_n;\ f,\mathbf{L}(n))=\{S_{xy}(\theta_n,\varphi_n;\ f,\mathbf{L}(n));\ x,y=\{\theta,\varphi\}\}$ is the scattering matrix, respectively, while,

$$\mathbf{E}_F(\theta_n,\varphi_n;\ f)=\frac{|\mathbf{r}_F|}{|\mathbf{r}_n-\mathbf{r}_F|}\frac{E_F(\theta_n,\varphi_n;\ f)}{E_F(0,0;\ f)}\times\exp(jk_0|\mathbf{r}_n-\mathbf{r}_F|-|\mathbf{r}_F|)[\cos\varphi_n\boldsymbol{\theta}+\sin\varphi_n\boldsymbol{\varphi}],\quad(2)$$

is the field pattern radiated by the feed on the nth element, $\mathbf{r}_F$ and $E_F(\theta,\varphi,f)$ being the feeder position and the element factor, respectively. We can see that the scattering matrix $\mathcal{S}(\theta_n,\varphi_n;\ f,\mathbf{L}(n))$ is largely dependent on the shape of the RA cells, exhibits a high degree of nonlinearity, and has no closed-form expression [15] that can be directly utilized. In this case, we need to find an evaluation function $\tilde{S}(\boldsymbol{z})$, that maps the input space $\mathbb{Z}$ to a high-dimensional space in which the linear function $\mathcal{S}(\mathbf{z})$ can be used to accurately perform the regression. To be exact, it is to find an evaluation function such that $\tilde{S}(\boldsymbol{z})\approx S(\boldsymbol{z})$, $\mathbf{z}\in\mathbb{Z}$, where $\mathbf{z}$ is the input vector of I+3 dimension which is defined by the incidence angles θ and φ, the working frequency f and the geometric parameters of I DoFs. The definition of input space $\mathbb{Z}$ is as follows:

$$\mathbb{Z}\triangleq\{\theta\in[\theta_{\min},\theta_{\max}];\varphi\in[\varphi_{\min},\varphi_{\max}];\ f\in[f_{\min},f_{\max}];\ L^{(i)}\in[L^{(i)}_{\min},L^{(i)}_{\max}]\}\ (i=1,...,I).\quad(3)$$

III. RESPONSE PREDICTION OF UNIT CELL BASED ON SVR

In this work, SVR is applied to find a surrogate model [16] to accommodate the inputs of the RA antenna unit cells. In order to find the mapping between the input $\mathbf{z}$ and the EM response output function $\tilde{S}(\boldsymbol{z})$, the elevation θ, the azimuth φ, the working frequency f, and the I DoFs of the array element are first discretized in A $[\theta_a=\theta_{\min}+(a-1)\Delta\theta;\ a=1,\ldots,A;\ \Delta\theta=(\theta_{\max}-\theta_{\min})/(A-1)]$, B $[\varphi_b=\varphi_{\min}+(b-1)\Delta\varphi;\ b=1,...,B;\ \Delta\varphi=(\varphi_{\max}-\varphi_{\min})/(B-1)]$, C $[f_c=f_{\min}+(c-1)\Delta f;\ c=1,\ldots,C;\ \Delta f=(f_{\max}-f_{\min})/(C-1)]$, and D $[L^{(i)}_{l_i}=L^{(i)}_{\min}+(d_i-1)\Delta L^{(i)},\ d_i=1,...,D_i;\ i=1,...,I;\Delta L^{(i)}=(L^{(i)}_{\max}-L^{(i)}_{\min})/(D_i-1)]$ quantized values, respectively (D indicates the total number of patch geometric shapes after removing the overlapping part of the ring patch). In this way, an FW simulation is performed for each mth $(m=1,...,M,\ M=A\times B\times C\times D)$ unit cell. Given an input $\mathbf{z}_m$ $[\mathbf{z}_m\triangleq[\theta_a,\varphi_b,f_c,\mathbf{L}_d]$, corresponding output $\mathcal{S}(\mathbf{z}_m)$ will be obtained, aiming at establishing the *sample set* $\mathcal{Q}\triangleq\{\mathbf{z}_m,\mathcal{S}(\mathbf{z}_m);\ m=1,...,M\}$ required for SVR training model. Although FW simulation can be used to calculate function $\mathcal{S}(\mathbf{z})$ simply and accurately, since the number of LUTs increases exponentially with the increase of DoFs [6], it is necessary to consider the storage and calculation time $T^{\mathrm{FW}}_{\mathrm{all}}$ of the simulation of unit cells with complex shapes ($T^{\mathrm{FW}}_{\mathrm{all}}\triangleq M\times T^{\mathrm{FW}}_{\mathrm{sin}}$, $T^{\mathrm{FW}}_{\mathrm{sin}}$ is the time taken to calculate a single $\mathcal{S}$ matrix).

To solve the problem of database storage and computing time, the machine learning method based on SVR is proposed in this paper. Getting an accurate prediction of the output $\tilde{S}(\boldsymbol{z})$, a certain number of samples should be randomly selected from the *sample set* simulated by FW for SVR learning, which is called

the *training set* $\mathcal{T} \triangleq \{\mathbf{z}_k, \mathrm{S}(\mathbf{z}_k); k = 1,...,K\}$. After the corresponding relationship between input and output is established by SVR, the EM response of the RA can be obtained quickly and accurately given any test data that is not in the training sample.

In the next section, the performance of the RA EM response estimation problem is also evaluated from the aspects of calculation error and time saved. The matrix norm error Ξ_1 and the phase mean squared error Ξ_2 are given by [7,17]:

$$\Xi_1 \triangleq \frac{1}{R}\sum_{r=1}^{R}\frac{\left\|\mathcal{S}^{\mathrm{SVR}}(\mathbf{z}_r)-\mathcal{S}(\mathbf{z}_r)\right\|^2}{\left\|\mathcal{S}(\mathbf{z}_r)\right\|^2}, \tag{4}$$

where $\mathcal{S}$ denotes the exact FW-computed scattering matrix, $\|\cdot\|$ being ℓ_2-norm, $R = M - K (r = 1,...,R)$ indicates the number of samples in the *testing set*, and,

$$\Xi_2 = \frac{1}{4R}\sum_{r=1}^{R}\sum_{\{x,y\}=\{\theta,\varphi\}}\left|\frac{1}{\pi}\arg\left[\frac{\mathcal{S}_{\mathrm{xx}}^{\mathrm{SVR}}(\mathbf{z}_r)}{\mathcal{S}_{\mathrm{xx}}(\mathbf{z}_r)}\right]\right|^2, \tag{5}$$

where the π normalization accounts for the fact that the phase is expressed in radians, whereas the coefficient 1/4 refers to the four entries of the scattering matrix. These metrics can quantitatively evaluate the prediction accuracy of method (4) and its reliability in estimating the phase of the scattering matrix (5) [7,17]. Another noteworthy evaluation factor is the computational efficiency, that is, the time saved by SVR compared to the FW simulation, given by:

$$\Delta T \triangleq 1 - \left|\frac{T_{\mathrm{train}}^{\mathrm{SVR}} + T_{\mathrm{test}}^{\mathrm{SVR}}}{T_{\mathrm{set}}^{\mathrm{FW}}}\right|, \tag{6}$$

where $T_{\mathrm{set}}^{\mathrm{FW}} \triangleq R \times T_{\mathrm{sin}}^{\mathrm{FW}}$ is the time for FW-computing the R items of *testing set*, $T_{\mathrm{train}}^{\mathrm{SVR}}$ is the time for the SVR training process, and $T_{\mathrm{test}}^{\mathrm{SVR}}$ (can be ignored) is the time for the SVR testing process.

Plus, two important evaluation indicators used for regression analysis, the determination coefficient (R^2) and the root mean square error (RMSE) are defined as follows:

$$R^2 = 1 - \frac{\sum_r^R \left(S^{\mathrm{SVR}}(\mathbf{z}_r) - S(\mathbf{z}_r)\right)^2}{\sum_r^R \left(S(\mathbf{z}_r) - \mathrm{mean}(S(\mathbf{z}_r))\right)^2}, \tag{7}$$

$$\mathrm{RMSE} = \sqrt{\frac{1}{R}\sum_r^R \left(S^{\mathrm{SVR}}(\mathbf{z}_r) - S(\mathbf{z}_r)\right)^2}, \tag{8}$$

where mean(·) represents the average.

IV. NUMERICAL RESULTS

In this paper, the scattering matrix of a RA element printed on a single-layer dielectric substrate with lattice period is studied, in which the thickness of the dielectric substrate is 1.524*mm*, the complex relative permittivity is $\varepsilon_r = 2.2 - j1.98\times10^{-2}$ ($\mathbf{d}_1 = (\lambda_0/3)\mathbf{x}$, $\mathbf{d}_2 = (\lambda_0/3)\mathbf{y}$ [see Fig. 2], λ_0 being the wavelength at the central frequency f_0), and the patch shape is multiple concentric square metal slots [i.e., the "Squared Phoenix" cell] [1,9,18]. The EM response calculation of the RA characterized by I = 4 DoFs is first discretized according to the following steps — $\theta_{\min} = 0$ [deg], $\theta_{\max} = 40$ [deg], $A = 5, \varphi_{\min} = 0$ [deg], $\varphi_{\max} = 45$ [deg], $B = 4$, $f_{\min} = 0.9 f_0$, $f_{\max}$ =1.1f_0, $C = 3$, $L_{\min}^{(1)} = 0.10\lambda_0$, $L_{\max}^{(1)} = 0.30\lambda_0$, $L_{\min}^{(2)} = 0.09\lambda_0$, $L_{\max}^{(2)} = 0.25\lambda_0$, $L_{\min}^{(3)} = 0.04\lambda_0$, $L_{\max}^{(3)} = 0.2\lambda_0$, $L_{\min}^{(4)} = 0.03\lambda_0$, $L_{\max}^{(4)} = 0.15\lambda_0$, $D_i = 5$ ($i = 1,...,I$). Excluding the overlapping parts of the concentric metal slots, the total number of geometric shapes is D = 120. The training samples required for the SVR are obtained by CST simulation modeling. Through CST simulation modeling, the total number of items in the *sample set* $\mathcal{Q}$ is M=7200.

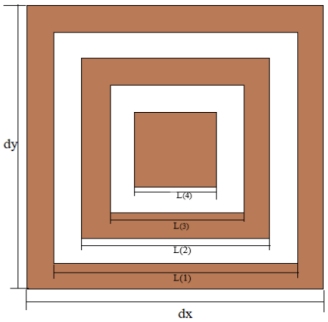

Fig. 2. Geometry of I=4 "Square Phoenix" unit cell.

The 7200 data generated by the FW simulation were divided into two subsets: a *training set* consisting of 6000 samples and a *testing set* which consists of 1200 samples. The inputs of SVR are the elevation θ_a, the azimuth φ_b, the frequency f_c, and I DoFs of geometric shapes, and the outputs are the magnitude, the phase, the real part and the imaginary part of the co-polarization $S_{\theta\theta}(\mathbf{z})$ and cross-polarization $S_{\theta\varphi}(\mathbf{z})$, respectively. The LIBSVM library [19] with the Gaussian kernel is used to get the SVR model. Two important parameters involved in SVR strategy—the penalty factor C and γ (γ is the parameter that comes with the kernel function), can be obtained by cross-validation and mesh parameter optimization [20], as shown in Table 1.

Table 1: The penalt factor C and $1/\gamma$ of SVR obtained by cross-validation

	Co-polarization		Cross-polarization	
	C	$1/\gamma$	C	$1/\gamma$
Magnitude	18	0.707	816	1.212
Phase	724	0.128	924	2.507
Real part	141	0.500	544	0.771
Imaginary part	364	0.911	512	0.354

Under the same conditions, the RBF method with simple network topology and fast learning speed is used as a comparison to illustrate the effectiveness of the proposed method. This paper calls the NEWRB toolbox function built in MATLAB to predict the EM response of RA antenna unit cell. Given that RBF and SVR are modeled under the same conditions, the maximum number of neural units in the RBF hidden layer is the total number of training data sets.

For verifying the validity of the proposed method, a sample that is not belong to $\mathcal{T}$ is randomly selected for numerical verification. Figures 3 (a) and 3 (b) show the plots of the magnitude and phase of $S_{\theta\theta}(\mathbf{z})$ versus the elevation θ when $f = f_0$ and φ=45 [deg], $L^{(1)} = 0.19\lambda_0$, $L^{(2)} = 0.16\lambda_0$, $L^{(3)} = 0.07\lambda_0$, $L^{(4)} = 0.05\lambda_0$. We can observe from the plot, compared with the RBF prediction method, as the elevation angle changes, the SVR is closer to the true value in predicting the scattering magnitude and phase.

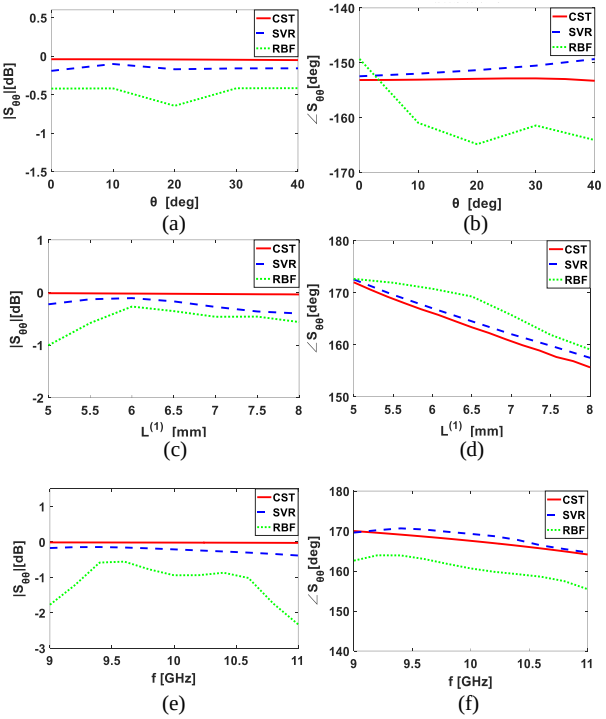

Fig. 3. Behavior of (a), (c), and (e) magnitude and (b), (d), and (f) phase of $S_{\theta\theta}(\mathbf{z})$ versus changes in (a) and (b) elevation angle θ, (c) and (d) element size [i.e., $L^{(1)}$], and (e) and (f) frequency.

The same consideration is given to the magnitude and phase of the EM response vary with the cell size [Figs. 3 (c), (d)] and frequency [Figs. 3 (e), (f)] of the element (where θ is 0 [deg]), we can see from the plots that the prediction results of SVR are also more accurate than that of RBF. As we expected, in these comparisons, using SVR to predict the EM response of a RA antenna element with a complex shape is significantly better than the predicted value of RBF in terms of prediction accuracy.

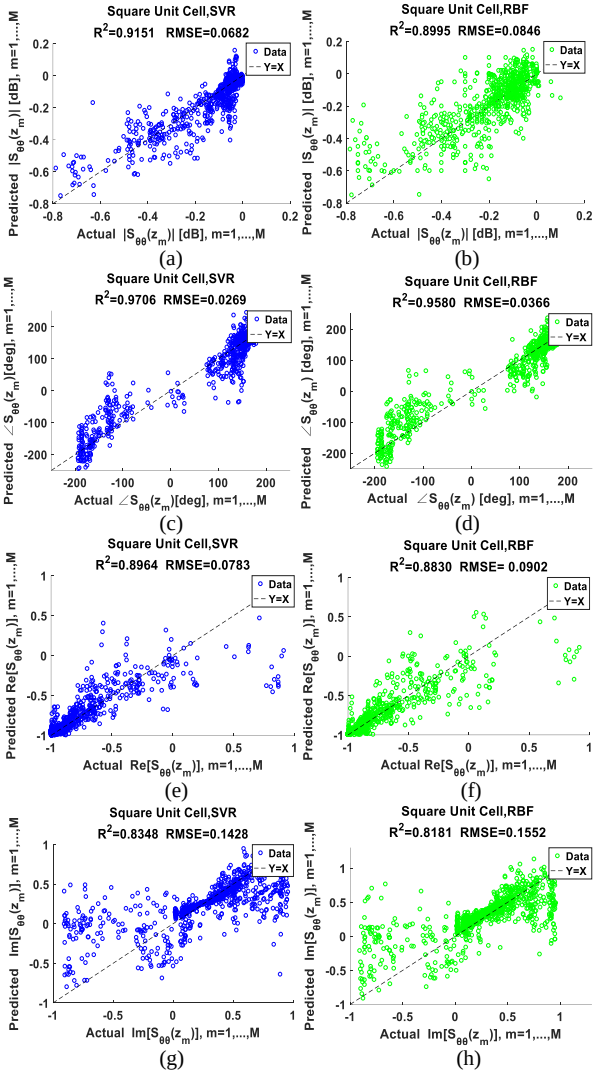

Fig. 4. Actual versus estimated values of (a) and (b) $|S_{\theta\theta}(\mathbf{z}_m)|$, (c) and (d) $\angle S_{\theta\theta}(\mathbf{z}_m)$, (e) and (f) $\mathrm{Re}[S_{\theta\theta}(\mathbf{z}_m)]$, and (g) and (h) $\mathrm{Im}[S_{\theta\theta}(\mathbf{z}_m)], m = 1,\ldots,M$, when using (a), (c), (e), and (g) SVR and (b), (d), (f), and (h) RBF prediction method.

Owing to the scattering coefficient is a complex number, the magnitude and phase of the scattering coefficient can be directly obtained from the real part and the imaginary part. Therefore, with purpose of further evaluating the enthusiasm of the SVR, it is also necessary to establish a training model of the real part and the imaginary part of the scattering coefficient by using SVR. Figure 4 shows the scatter plots of the magnitude [Figs. 4 (a), (b)], the phase [Figs. 4 (c), (d)],

the real part [Figs. 4 (e), (f)], and the imaginary part [Figs. 4 (g), (h)] of $S_{\theta\theta}(\mathbf{z}_m), m=1,...,M$, with the line Y = X representing the ideal bisector. The more concentrated the scatter is on the ideal bisector, the higher the accuracy predicted. From the scatter distribution in Fig. 4 and the determination coefficient R^2 and RMSE calculated by formulas (7) and (8), we can see that the SVR can accurately predict the EM response of RA antenna element with complex shapes, which are closer to the ideal bisector than the RBF ones [Figs. 4 (b), (d), (f), and (h)]. In addition, $\Xi_1^{\mathrm{SVR}}=0.0788$ and $\Xi_2^{\mathrm{SVR}}=0.0223$ versus $\Xi_1^{\mathrm{RBF}}=0.0862$ and $\Xi_2^{\mathrm{RBF}}=0.0477$, calculated by formulas (4) and (5) can be more explained. It is worth mentioning that SVR greatly improves the calculation efficiency of the EM response of the RA, $\Delta T^{\mathrm{SVR}}=0.15$ ($T_{\mathrm{sin}}^{\mathrm{FW}}\approx 1.20\times 10^{2}[\mathrm{s}]$) can be obtained from formula (6), that is to say, 15% time is saved compared with FW simulation. Similarly, time savings using the RBF method can also be obtained, $\Delta T^{\mathrm{RBF}}=0.70$, 70% time is saved (The training time of RBF is $T_{\mathrm{train}}^{\mathrm{RBF}}\approx 4.32\times 10^{4}[\mathrm{s}]$). From the perspective of quantitative indicators, in terms of time savings, there is no doubt that the SVR is more time-saving than the FW simulation in predicting EM response of the RA, but it is slightly inferior to the RBF, because the SVR needs to use mesh parameter optimization and cross-validation to find the optimal values of C and γ , while RBF is not needed.

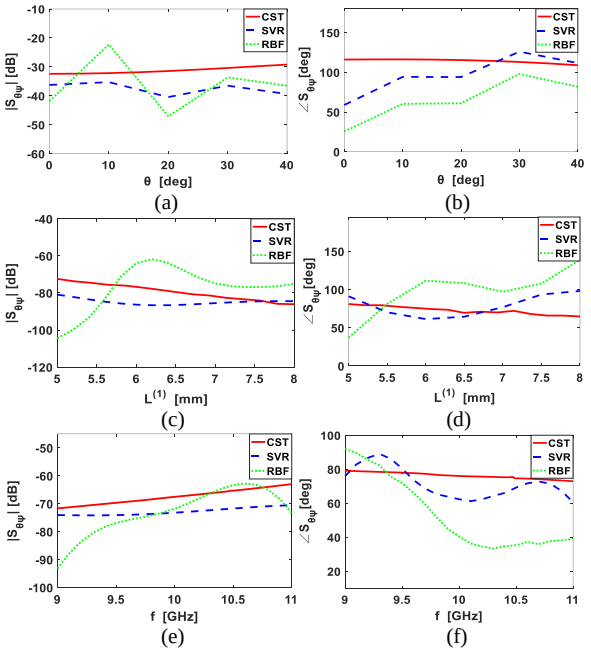

Fig. 5. Behavior of (a), (c), and (e) magnitude and (b), (d), and (f) phase of $S_{\theta\varphi}(\mathbf{z})$ versus changes in (a) and (b) incidence angle θ, (c) and (d) element size [i.e., $L^{(1)}$], and (e) and (f) frequency.

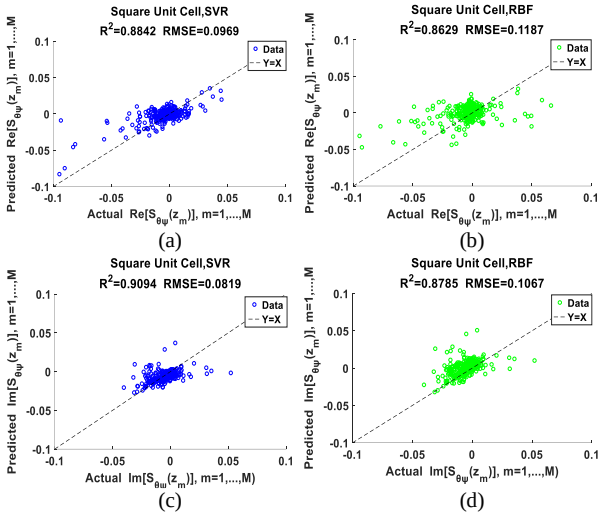

Fig. 6. Actual versus estimated values of (a) and (b) $\mathrm{Re}[S_{\theta\varphi}(\mathbf{z}_m)]$, and (c) and (d) $\mathrm{Im}[S_{\theta\varphi}(\mathbf{z}_m)], m=1,...,M$, when using (a) and (c) SVR, and (b) and (d) RBF prediction method.

Cross-polarization component $S_{\theta\varphi}(\mathbf{z}_m), m=1,...,M$ is also very important for the performance analysis of RA antenna. We can clearly see from the Figs. (5) and (6) that the RBF results deviate significantly from the ideal curve for both the curve that varies with a single input variable (Fig. 5) or the scatter cloud (Fig. 6), and the proposed method is significantly better than the predicted value of RBF. Similarly, the corresponding prediction errors of $S_{\theta\varphi}(\mathbf{z}_m), m=1,...,M$ can be obtained from formulas (4) and (5), namely $\Xi_1^{\mathrm{SVR}}=0.1021$ and $\Xi_2^{\mathrm{SVR}}=0.1764$ versus $\Xi_1^{\mathrm{RBF}}=0.1288$ and $\Xi_2^{\mathrm{RBF}}=0.1953$. Although the cross-polarization scattering characteristics of the "*Square Phoenix*" unit cells are weaker than the co-polarization scattering characteristics [18], from these quantitative indicators and Fig. 5 and Fig. 6, it is sufficient to prove the applicability of the proposed method to the EM response prediction of complex RA antenna elements.

V. CONCLUSION

In this letter, an effective and accurate prediction methodology, a machine learning method based on SVR is proposed to predict the EM response of complex RA antenna elements. The original arbitrary number of DoFs passive EM scattering problems is transformed into a regression estimation problem, and scattering model is established by using SVR through appropriate offline training, which overcomes the problems of traditional FW simulation and database. The calculation of the magnitude and phase of the scattering coefficient shows that the SVR and the FW simulation results are in good agreement (see Fig. 3), even for the cross-coefficient (see

Fig. 5), although they are highly nonlinear, which is very difficult to model. Through the quantitative calculation of equations (4) and (5), it is strongly demonstrated that compared with the ANNs algorithm based on RBFN, the EM response of complex RA antennas can be predicted more accurately by SVR. Although the time saved by SVR is second to RBFN, it is also more efficient than the FW simulation algorithm. With flexible tradeoff accuracy and computational efficiency, SVR can provide reliable, accurate and fast estimation of EM response, and providing an effective way to solve EM scattering problems.

ACKNOWLEDGMENT

This work was supported by the National Natural Science Foundation of China under Grant 61771008.

REFERENCES

[1] R. Deng, F. Yang, S. Xu, and M. Li, "A low-cost metal-only reflectarray using modified slot-type Phoenix element with 360◦ phase coverage," *IEEE Trans. Antennas Propag*., vol. 64, no. 4, pp. 1556-1560, Apr. 2016.

[2] J. Huang and J. A. Encinar, *Reflectarray Antennas*. Piscataway, NJ, USA: Wiley, 2008.

[3] D. R. Prado, M. Arrebola, M. R. Pino, R. Florencio, R. R. Boix, J. A. Encinar, and F. Las-Heras, "Efficient crosspolar optimization of shaped- beam dual-polarized reflectarrays using full-wave analysis for the antenna element characterization," *IEEE Transactions on Antennas and Propagation*, vol. 65, no. 2, pp. 623-635, 2017.

[4] R. Florencio, R. R. Boix, and J. A. Encinar, "Enhanced MoM analysis of the scattering by periodic strip gratings in multilayered substrates," *IEEE Trans. Antennas Propag*., vol. 61, no. 10, pp. 5088-5099, Oct. 2013.

[5] F. Gunes, S. Nesil, and S. Demirel, "Design and analysis of Minkowski reflectarray antenna using 3-D CST Microwave Studio-based neural network model with particle swarm optimization," *Int. J. RF Microw. Comput. Eng*., vol. 23, no. 2, pp. 272-284, Mar. 2013.

[6] L. Marnat, R. Loison, R. Gillard, D. Bresciani, and H. Legay, "Accurate synthesis of a dual linearly polarized reflectarray," in Proc. *3rd Eur. Conf. Antennas Propag. (EuCAP)*, Berlin, Germany, pp. 2523-2526, 2009.

[7] M. Salucci, L. Tenuti, G. Oliveri, and A. Massa, "Efficient prediction of the EM response of reflectarray antenna elements by an advanced statistical learning method," *IEEE Trans. Antennas Propag.*, vol. 66, no. 8, pp. 3995-4007, Aug. 2018.

[8] M. de Berg, O. Cheong, M. van Kreveld, and M. Overmars, *Computational Geometry: Algorithms and Applications*. Santa Clara, CA, USA: Springer-Verlag, 2008.

[9] R. Deng, S. Xu, F. Yang, and M. Li, "Single-layer dual-band reflectarray antennas with wide frequency ratios and high aperture efficiencies using Phoenix elements," *IEEE Trans. Antennas Propag*., vol. 65, no. 2, pp. 612-622, Feb. 2017.

[10] C. Shan, X. Chen, H. Yin, W. Wang, G. Wei, and Y. Zhang, "Diagnosis of calibration state for massive antenna array via deep learning," *IEEE Wireless Communications Letters*, vol. 8, no. 5, pp. 1431-1434, Oct. 2019.

[11] J. Cai, C. Yu, J. Xia, L. Sun, S. Chen, B. Pan, J. Su, and J. Liu, "Support Vector Regression Based Behavioral Model for Load Mismatched PAs," *2019 IEEE International Symposium on Radio-Frequency Integration Technology (RFIT)*, Nanjing, China, pp. 1-3, 2019.

[12] H. M. Yao, W. E. I. Sha, and L. Jiang, "Two-step enhanced deep learning approach for electromagnetic inverse scattering problems," *IEEE Antennas and Wireless Propagation Letters*, vol. 18, no. 11, pp. 2254-2258, Nov. 2019.

[13] V. Richard, R. Loison, R. Gillard, H. Legay, and M. Romier, "Loss analysis of a reflectarray cell using ANNs with accurate magnitude prediction," in *11th European Conference on Antennas and Propagation (EuCAP)*, Paris, France, pp. 2402-2405, Mar. 2017.

[14] D. M. Pozar, S. D. Targonski, and H. D. Syrigos, "Design of millimeter wave microstrip reflectarrays," *IEEE Trans. Antennas Propag.*, vol. 45, no. 2, pp. 287-296, Feb. 1997.

[15] P. Rocca, L. Poli, N. Anselmi, M. Salucci, and A. Massa, "Predicting antenna pattern degradations in microstrip reflectarrays through interval arithmetic," *IET Microw., Antennas Propag*., vol. 10, no. 8, pp. 817-826, Mar. 2016.

[16] A. I. J. Forrester, A. Sóbester, and A. J. Keane, *Engineering Design via Surrogate Modelling: A Practical Guide*. New York, NY, USA: Wiley, 2008.

[17] Y. Mao, S. Xu, F. Yang, and A. Z. Elsherbeni, "A novel phase synthesis approach for wideband reflectarray design," *IEEE Trans. Antennas Propag*., vol. 63, no. 9, pp. 4189-4193, Sep. 2015.

[18] L. Moustafa, R. Gillard, F. Peris, R. Loison, H. Legay, and E. Girard, "The Phoenix cell: A new reflectarray cell with large bandwidth and rebirth capabilities," *IEEE Antennas Wireless Propag. Lett.*, vol. 10, pp. 71-74, Jan. 2011.

[19] C.-C. Chang and C.-J. Lin, "LIBSVM: A library for support vector machines," *ACM Trans. Intell. Syst. Technol*., vol. 2, no. 3, pp. 27:1-27:27, Apr. 2011, software available at http://www.csie.ntu.edu.tw/_cjlin/libsvm

[20] G. C. Cawley and N. L. C. Talbot, "Efficient leave-one-out cross-validation of Kernel fisher discriminant classifiers," [J]. *Pattern Recognition*, vol. 11, 2003.